Astronomy & Astrophysics manuscript no.
(will be inserted by hand later)

The CORALIE survey for southern extrasolar planets V. 3 new extrasolar planets⋆

D. Naef[1], M. Mayor[1], F. Pepe[1], D. Queloz[1], N.C. Santos[1], S. Udry[1], and M. Burnet[1]

Observatoire de Genève, 51 ch. des Maillettes, CH–1290 Sauverny, Switzerland

Received / Accepted

Abstract. We report the detection of 3 new planetary companions orbiting the solar-type stars GJ 3021, HD 52265 and HD 169830 using radial-velocity measurements taken with the CORALIE echelle spectrograph. All these planetary companions have longer orbital periods than the 51 Peg-like objects. The orbits are fairly eccentric. The minimum masses of these planets range from 1 to 3.3 M_{Jup}. The stars have spectral types from F8V to G6V. They are metal-rich. We also present our radial-velocity measurements for three solar-type stars known to host planetary companions ι Hor (HD 17051), HD 210277 and HD 217107.

Key words. techniques: radial velocities – stars: individuals: GJ 3021 – stars: individuals: HD 52265 – stars: individuals: HD 169830 – stars: planetary systems

1. Introduction

Less than six years after the discovery of the first extrasolar planet orbiting the star 51 Peg (Mayor & Queloz 1995), the number of extrasolar planets detected around solar-type stars is now reaching 63 (minimum masses below 10 M_{Jup}). None of the planetary companions detected so far resembles the giant planets of the solar system. The increase of the precision as well as the increase of the duration of the surveys make the radial-velocity searches sensitive to long period and very low mass companions. Sub-Saturnian planets have been recently detected (Marcy et al. 2000, May the 4th 2000 ESO PR[1]). We find in the highlights of this research domain the detection of a 3-planet system orbiting υ And (Butler et al. 1999), the detection of a 2-Saturnian planet system orbiting HD 83443 (Mayor et al. 2000) and the detection of the photometric (Charbonneau et al. 2000; Henry et al. 2000) and spectroscopic (Queloz et al. 2000a) transits of the extrasolar planet orbiting the star HD 209458. Planetary companions have also been detected in wide binary systems: see e.g. 16 Cyg B (Cochran et al. 1997), GJ 86 (Queloz et al. 2000d) or HD 80606 (Naef et al. 2001). It is interesting to notice as well that the majority of the stars with planets have a higher metal content than field stars in the solar vicinity (Gonzalez 2000; Santos et al. 2000a,c, 2001c).

Some of the detected planets have short periods and very small orbital separations (the "Hot Jupiters"). Most of these Hot Jupiters are on circular orbits. There are also longer period objects. The orbital eccentricities of these objects almost cover the full possible range: from nearly circular (see e.g. the recently announced planet around HD 28185, April the 4th 2001 ESO PR[2]) to nearly unity as in the case of HD 80606 (Naef et al. 2001). The 3 new extrasolar planet candidates we present in Sect. 2 belong to this kind of objects (Jovian masses, longer periods, elongated orbits).

In this paper, we present the radial-velocity data obtained with CORALIE for the stars GJ 3021, HD 52265[3] and HD 169830. They reveal the presence of Jovian-mass companions. Section 2.2 describes the basic stellar properties of these stars. The Lithium abundances and the chromospheric activity of these objects are discussed in Sect. 2.3 and 2.4. The orbital solutions are presented in Sect. 2.5. In Sect. 3, we present our radial-velocity measurements for the stars ι Hor, HD 210277 and HD 217107.

2. Extrasolar planets orbiting the stars GJ 3021, HD 52265, and HD 169830

Send offprint requests to: Dominique Naef, e-mail: dominique.naef@obs.unige.ch

⋆ Based on data obtained with the CORALIE echelle spectrograph mounted on the 1.2-m "Leonard Euler" Swiss telescope at ESO-La Silla Observatory (Chile)

[1] www.eso.org/outreach/press-rel/pr-2000/pr-13-00.html

[2] www.eso.org/outreach/press-rel/pr-2001/pr-07-01.html

[3] The detection of the planetary companion around HD 52265 was independently announced during the writing of this paper by Butler et al. (2000)

Table 1. Planetary and brown dwarf candidates detected with CORALIE

Star	Reference
GJ 86	Queloz et al. 2000d
HD 75289	Udry et al. 2000a
HD 130322	Udry et al. 2000a
HD 192263	Santos et al. 2001a, 2000d
GJ 3021	Naef et al. 2000, this paper
HD 168746	Pepe et al. in prep.
HD 83443b	Mayor et al. 2000
HD 108147	Pepe et al. in prep.
HD 52265	this paper
HD 82943b	Mayor et al. in prep.
HD 169830	this paper
HD 160202†	Udry et al. in prep
HD 202206†	Udry et al. in prep
HD 6434	Queloz et al. 2000b
HD 19994	Queloz et al. 2000b
HD 92788‡	Queloz et al. 2000b
HD 121504	Queloz et al. 2000b
HD 83443b	Mayor et al. 2000
HD 168443c	Udry et al. 2000b
HD 28185	Santos et al. in prep.
HD 82943c	Mayor et al. in prep.
HD 141937	Udry et al. in prep.
HD 213240	Santos et al. in prep.

† Low-mass brown dwarf
‡ Independently announced by Fischer et al. (2001)

2.1. CORALIE high-precision radial-velocity survey

Our radial-velocity measurements are done by computing the cross-correlation function (CCF) between the observed stellar spectrum and a numerical template. The instrumental velocity drifts are monitored and corrected using the "simultaneous Thorium referencing technique" with dual fibers (more details in Baranne et al. 1996). The achieved precision of this technique with CORALIE is currently of the order of 7-8 $\mathrm{m\,s^{-1}}$ for almost three years (Queloz et al. 2000c). Three years after the start of the *Geneva Southern Planet Search Programme* (Queloz et al. 2000c; Udry et al. 2000c,a) at ESO-La Silla Observatory (Chile), 21 planetary and 2 low-mass brown dwarf candidates have already been detected (see Table 1).

The 298 CORALIE individual radial-velocity measurements presented in this paper are available in electronic form at the CDS in Strasbourg.

2.2. Characteristics of the stars

2.2.1. GJ 3021

GJ 3021 (HD 1237, HIP 1292) is a bright G6 dwarf located in the southern constellation of Hydrus. The astrometric parallax from the HIPPARCOS satellite (ESA 1997) $\pi = 56.76 \pm 0.53$ mas sets the star at a distance of 17.6 pc from the Sun. The HIPPARCOS apparent magnitude and colour index are $m_V = 6.59$ and $B - V = 0.749$. Thus the absolute magnitude is $M_V = 5.36$. With a bolometric correction $B.C. = -0.16$ (Flower 1996), we find an effective temperature of $T_{\rm eff} = 5417$ K and a luminosity of $L = 0.66\,L_\odot$. Using HIPPARCOS proper motions and parallax and the γ velocity of GJ 3021, we find $(U, V, W) = (33.7,\ -17.4,\ 2.8)\ \mathrm{km\,s^{-1}}$. This velocity vector is similar to the one observed for stars in the Hyades Super-Cluster (Chereul et al. 1999).

In a recent paper, Santos et al. (2000c), using a high signal-to-noise CORALIE spectrum, derived the following atmospheric parameters for GJ 3021: $T_{\rm eff} = 5540 \pm 75$ K, $\log g = 4.7 \pm 0.2$ (cgs) and $[\mathrm{Fe/H}] = 0.1 \pm 0.08$. From the CORAVEL CCF dip width, we obtain the projected rotational velocity $v \sin i = 5.5 \pm 1\ \mathrm{km\,s^{-1}}$ (Benz & Mayor 1984). The calibration by Benz & Mayor (1984) does not account for metallicity effects. In their calibration, the intrinsic line width for non-rotating stars is supposed to be mainly a function of the $B - V$ colour index (pressure broadening by Van der Waals effect). For metal-rich stars, the number of saturated lines increases. This causes the CCF intrinsic width to increase. With the calibration by Benz & Mayor (1984), the intrinsic line width is therefore under-estimated and the rotational broadening over-estimated for metal-rich stars. The $v \sin i$ value indicated above is thus an upper-limit. The ROSAT All-Sky Survey X–ray luminosity for GJ 3021 is $L_X = 103.6 \cdot 10^{27}\ \mathrm{erg\,s^{-1}}$ (Hünsch et al. 1999).

GJ 3021 is not photometrically stable. The scatter of the HIPPARCOS photometric measurements is of the order of 12 mmag. In the HIPPARCOS catalogue, GJ 3021 is classified as a possible micro-variable star. The Fourier transform of the photometric data shows no clear significant frequency. It is not surprising, assuming that the photometric signal is due to features such as spots on the stellar surface. The typical lifetimes of spots are known to be much shorter than the duration of the HIPPARCOS mission.

Finally, no infrared excess was detected for GJ 3021 at 60 μm (ISO data, Decin et al. 2000). A CORALIE radial-velocity monitoring of a set of G dwarfs observed in the infrared by Decin et al. (2000) is on its way. The main goal of this combined survey is to study the correlation (or anti-correlation) between the presence of an infrared excess and the occurrence of planets or companion stars. In the selected sample, two stars actually have a planetary companion, GJ 3021 (this paper) and GJ 86 (Queloz et al. 2000d), without trace of infrared excess.

Observed and inferred stellar parameters are summarized in Table 2 with references to the corresponding observations or methods used to derive the quantities.

2.2.2. HD 52265

HD 52265 (HIP 33719) is a bright ($m_V = 6.29$) G0 dwarf located in the constellation of Monoceros (the Unicorn) 28.1 pc away from the Sun. Using the HIPPARCOS (ESA 1997) precise astrometric parallax ($\pi = 35.63 \pm 0.84$ mas), we infer an absolute magnitude of $M_V = 4.05$. This value,

Table 2. Observed and inferred stellar parameters for GJ 3021, HD 52265 and HD 169830. The spectral types, apparent magnitudes, color indexes, parallaxes and proper motions are from HIPPARCOS (ESA 1997). The bolometric correction is computed with the calibration by Flower (1996). The atmospheric parameters $T_{\rm eff}$, $\log g$, [Fe/H] and $\xi_{\rm t}$ are from Santos et al. (2000c). The X–ray luminosities are from Hünsch et al. (1999) for GJ 3021 and from Piters et al. (1998) for HD 169830. The projected velocities are derived from CORAVEL with the calibration by Benz & Mayor (1984). The ages and masses of HD 52265 and HD 169830 are derived from the Geneva evolutionary tracks (Schaerer et al. 1993)

Parameter	**Units**	**GJ 3021**	**HD 52265**	**HD 169830**
Sp. Type		G6V	G0V	F8V
$m_{\rm V}$		6.59	6.29	5.90
$B-V$		0.749 ± 0.004	0.572 ± 0.003	0.517 ± 0.004
π	(mas)	56.76 ± 0.53	35.63 ± 0.84	27.53 ± 0.91
Distance	(pc)	$17.62 \pm {}^{0.17}_{0.16}$	$28.07 \pm {}^{0.68}_{0.65}$	$36.32 \pm {}^{1.24}_{1.16}$
$\mu_\alpha \cos(\delta)$	(mas yr^{-1})	433.87 ± 0.53	−115.76 ± 0.68	−0.84 ± 1.23
μ_δ	(mas yr^{-1})	−57.95 ± 0.48	80.35 ± 0.55	15.16 ± 0.72
$M_{\rm V}$		5.36	4.05	3.10
B.C.		−0.16	−0.046	−0.02
L	($L_\odot$)	0.66	1.98	4.63
$T_{\rm eff}$	(°K)	5540 ± 75	6060 ± 50	6300 ± 50
$\log g$	(cgs)	4.70 ± 0.20	4.29 ± 0.25	4.11 ± 0.25
$\xi_{\rm t}$	(km s^{-1})	1.47 ± 0.10	1.29 ± 0.10	1.37 ± 0.10
[Fe/H]		0.10 ± 0.08	0.21 ± 0.06	0.21 ± 0.05
M_1	($M_\odot$)	0.9	1.18	1.4
R	($R_\odot$)	0.9	1.1	1.2
$L_{\rm X}$	(10^{27} erg s^{-1})	103.6	...	< 398
$v \sin i^\dagger$	(km s^{-1})	5.5 ± 1	5.2 ± 1	3.8 ± 1
Age	(Gyr)	...	3.5	2.3

† over-estimated for metal-rich stars, see Sect. 2.2.1

slightly above the main sequence, disagrees with the commonly assumed spectral classification G0 III-IV for this star. With the bolometric correction ($B.C. = -0.046$) and temperature scale calibrated by Flower (1996), we find an effective temperature $T_{\rm eff} = 5995$ K and a luminosity $L = 1.98\,L_\odot$.

With a high signal-to-noise CORALIE spectrum, Santos et al. (2000c) derived the following stellar atmospheric parameters for HD 52265: $T_{\rm eff} = 6060 \pm 50$ K, $\log g = 4.29 \pm 0.25$ (cgs) and [Fe/H] $= 0.21 \pm 0.06$. Using the Geneva stellar evolution models (Schaerer et al. 1993) with $T_{\rm eff} = 6060$ K, $M_{\rm V} = 4.05$ and [Fe/H] $= 0.21$, we measure a mass $M_1 = 1.18\,M_\odot$ and an age of 3.5 Gyr. HD 52265 appears to be a slightly evolved metal-rich G0 dwarf.

From CORAVEL measurements, we compute $v \sin i = 5.2 \pm 1$ km s^{-1} (Benz & Mayor 1984, over-estimated, see Sect. 2.2.1). Finally, HD 52265 is photometrically stable (HIPPARCOS photometry, ESA 1997). The main stellar characteristics of HD 52265 are summarized in Table 2.

2.2.3. HD 169830

HD 169830 (HIP 90485) is a bright ($m_{\rm V} = 5.9$) F8 dwarf located in the constellation of Sagittarius (the Archer) 36.3 pc away from the Sun. With the HIPPARCOS (ESA 1997) astrometric parallax ($\pi = 27.53 \pm 0.91$ mas), the bolometric correction ($B.C. = -0.19$) and the temperature scale calibrated by Flower (1996), we compute the absolute magnitude, the effective temperature and the luminosity of HD 169830: $M_{\rm V} = 3.10$, $T_{\rm eff} = 6211$ K and $L = 4.63\,L_\odot$. Using Strömgren photometry, Edvardsson et al. (1993) have inferred stellar atmospheric parameters for HD 169830. They found $T_{\rm eff} = 6382$ K, $\log g = 4.15$ (cgs), [M/H] $= 0.17$ and [Fe/H] $= 0.13$. With a high signal-to-noise CORALIE spectrum, Santos et al. (2000c) derived similar values for the atmospheric parameters ($T_{\rm eff} = 6300 \pm 50$ K, $\log g = 4.11 \pm 0.25$ (cgs) and [Fe/H] $= 0.21 \pm 0.05$). HD 169830 is a slow rotator. Using CORAVEL data, we have $v \sin i = 3.8 \pm 1$ km s^{-1} (Benz & Mayor 1984, over-estimated, see Sect. 2.2.1). Edvardsson et al. (1993) also estimated the age of HD 169830 using its position in a colour-magnitude diagram. They found an age of 2.2 Gyr. This value is in agreement with the 2 Gyr found by Ng & Bertelli (1998) and also consistent with the value obtained using the Geneva evolutionary tracks (Schaerer et al. 1993): $age = 2.3$ Gyr, $M_1 = 1.4\,M_\odot$.

Using data from the ROSAT All-Sky Survey, Piters et al. (1998) obtained an upper limit for the X–ray luminosity of HD 169830: $L_{\rm X} < 398 \cdot 10^{27}$ erg s^{-1}. A carefull analysis of the ROSAT data (M. Audard, priv. comm.) shows that there is no source at the position of the star. The X–ray flux value is consistant with the background noise. Note that there is a bright nearby X–ray source (the LMXB Sgr X–4) that could be responsible for the

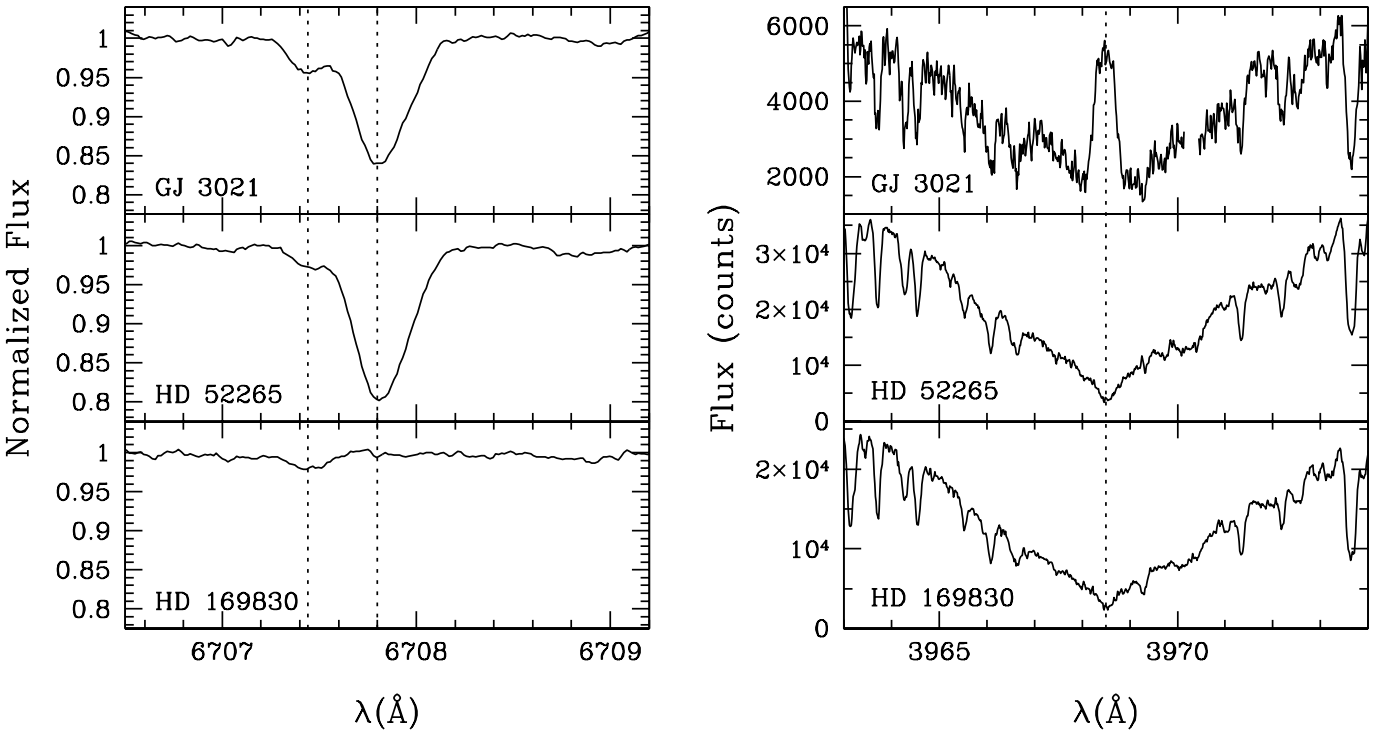

Fig. 1. Results of the addition of the CORALIE spectra. Left: The λ 6707.8 Å Li I absorption line region for GJ 3021, HD 52265 and HD 169830. The Lithium is clearly detected for GJ 3021 and HD 52265. The dotted lines indicate the positions of the λ 6707.4 Å Fe I and λ 6707.8 Å Li I lines. Right: the λ 3968.5 Å Ca II H absorption line region. A strong chromospheric emission is detected for GJ 3021. The two other candidates do not exhibit any trace of chromospheric emission

high X–ray background. The main stellar characteristics of HD 169830 are summarized in Table 2.

2.3. Lithium abundances

In this section, we estimate the Lithium abundance of the host stars with CORALIE spectra. In order to obtain a high signal in the λ 6707.8 Å Li I line region, we added all the measured spectra. The latter have been measured with our standard instrumental configuration. In this configuration, the Thorium-Argon lamp is used, adding a reference spectrum on the CCD. This reference spectrum is located between the orders of the stellar echelle spectrum. This configuration, needed for high-precision radial-velocity measurements, is not optimal for spectroscopic determinations (such as abundance determinations). However the spectra measured in this configuration are usable for limited spectroscopic determinations. The main interest of such determinations is the possibility of getting spectroscopic informations for very large stellar samples without specific measurements (i.e. without the need of additional observing time).

The two difficulties of this configuration for abundance determinations are: the additional background contamination and the shorter distance between the orders preventing us from correctly estimating the background contamination level. The measured fluxes are then not corrected for the background contamination effect. The obtained spectral lines have weaker contrasts and therefore smaller equivalent widths. The typical background contamination level measured for ELODIE (Baranne et al. 1996), a similar instrument, is about 3 % in the λ 6707.8 Å Li I line region. We have used this value to correct our equivalent width measurements.

We also used two GJ 3021 spectra taken without calibration lamp (single fiber mode) in order to check our correction scheme. In this case, the background contamination is corrected on the CCD frame. The corrected equivalent width measured with the calibration lamp (57.7 mÅ) is in good agreement with the value measured without calibration lamp (57.6 mÅ).

Figure 1 (left) shows the spectra we obtain after adding all the available spectra of GJ 3021, HD 52265 and HD 169830. The signal-to-noise ratio of these spectra is of the order of 300 at the continuum. The Lithium absorption feature is clearly visible for GJ 3021 and HD 52265. There are no clear traces of Lithium for HD 169830. The λ 6707.4 Å Fe I absorption feature is clearly visible for the 3 stars on the blue edge of the Lithium line. Table 3 shows the results of double gaussian fits to the Fe I–Li I blend for GJ 3021 and HD 52265.

To estimate the Lithium abundance, we have used the curves of growth tabulated by Soderblom et al. (1993) computed for the Pleiades metallicity. The Lithium abundances then obtained from our equivalent widths are listed in Table 3 (on a scale where $\log n(\mathrm{H}) = 12$). Our deter-

Table 3. Results of double-gaussian fits to the Fe I-Li I blend and Lithium abundances for GJ 3021 and HD 52265. $W_{\lambda,\rm cor}$ is the equivalent width corrected for the assumed 3 % background contamination level. The values in parentheses after the abundance values indicate the change in $\log n(\rm Li)$ resulting from a 1σ change in the effective temperature without accounting for other error sources. More realistic errors are probably not better than 0.1-0.15 dex. Note the good agreement between our abundances and the values by Israelian et al. (in prep.)

		GJ 3021	**HD 52265**
		Fe I Line	
λ	Å	6707.438	6707.441
$W_{\lambda,\rm cor}$	mÅ	8.38	3.97
		Li I Line	
λ	Å	6707.832	6707.837
$W_{\lambda,\rm cor}$	mÅ	57.56	69.33
$T_{\rm eff}$	K	5540 ± 75	6060 ± 50
$\log W_{\lambda,\rm cor}$	mÅ	1.76	1.84
$\log n(\rm Li)$		2.11 (0.08)	2.70 (0.04)
$\log n(\rm Li)^\dagger$		2.11	2.77

† Israelian et al. (in prep.)

mination of the Lithium abundance for GJ 3021 corresponds to the typical Lithium abundance measured for G6 dwarfs in the Hyades (see e.g. Soderblom et al. 1993). For HD 169830, an upper limit of the Lithium equivalent width can be estimated. We have (2σ confidence level): $W_\lambda < 2\,(\rm S/N)^{-1}\,\Sigma\,\sqrt{2\pi}$ where Σ is a typical line width. With $\rm S/N = 300$ and $\Sigma = 130$ mÅ, we have: $W_\lambda < 2.17$ mÅ. Correcting this value for the background contamination, we have $W_{\lambda,\rm max} = 2.24$ mÅ. This value provides the following constraint on the Lithium abundance of HD 169830: $\log n(\rm Li) < 1.31$ (2σ confidence level).

Our determinations agree with a recent study by Israelian et al. (in prep.). The values they obtained for GJ 3021 and HD 52265 are respectively $\log n(\rm Li) = 2.11$ and 2.77. They also obtained an upper limit for the Lithium abundance of HD 169830: $\log n(\rm Li) < 1.12$.

2.4. Chromospheric activity

Figure 1 (right) shows the λ 3968.5 Å Ca II H absorption line region for GJ 3021, HD 52265 and HD 169830. These spectra were obtained by adding all our CORALIE spectra. We have derived the $\log(R'_{\rm HK})$ chromospheric activity indicator for the three primary stars (see Santos et al. 2001b, 2000e for details about the technique). Table 4 shows the results: HD 52265 and HD 169830 are chromospherically inactive and GJ 3021 is very active. For the latter, we find $\log(R'_{\rm HK}) = -4.27$, a value substantially higher than the one by Henry et al. (1996, $\log(R'_{\rm HK}) = -4.44$) whose result is based on only one measurement without estimation of the scatter. We believe that given our estimate of the scatter, the discrepancy between the two values is due to the variability of the activity level of GJ 3021.

Table 4. Measured chromospheric activity for the three primary stars using CORALIE spectra. $N_{\rm meas}$ indicates the number of usable spectra. $S_{\rm COR}$ is the activity index obtained with CORALIE. Activity values have been calibrated to the Mount-Wilson system (Vaughan et al. 1978) before computing the $\log(R'_{\rm HK})$ indicator so that it can be compared to the values by Henry et al. (1996). Notice the high $S_{\rm COR}$ derived for GJ 3021 and the large dispersion around this mean value

Star	$N_{\rm meas}$	$S_{\rm COR}$	$\sigma(S_{\rm COR})$	$\log(R'_{\rm HK})$
GJ 3021	20	0.578	0.11	−4.27
HD 52265	31	0.146	0.03	−4.91
HD 169830	11	0.136	0.02	−4.93

With the $\log(R'_{\rm HK})$ value, we can estimate the rotational periods (using the calibration in Noyes et al. 1984) and the stellar ages (using the calibration in Donahue 1993 also quoted in Henry et al. 1996). The rotational periods we obtain for HD 52265 and HD 169830 are 14.6 and 9.5 days, respectively and ages of 4 Gyr for both stars. For GJ 3021, the scatter of our activity measurements is large (see Table 4). With our mean activity value $\log(R'_{\rm HK}) = -4.27$, we derive a rotational period of 4.1 days and an age of 0.02 Gyr. Estimates of the maximum rotational period and age can be obtained by using our lowest activity value $\log(R'_{\rm HK}) = -4.49$ yielding $P_{\rm rot,max} = 12.6$ days and $Age_{\rm max} = 0.8$ Gyr. This maximum age estimate is compatible with the age of the Hyades.

2.5. Orbital solutions

61 and 35 CORALIE high precision radial-velocity measurements are available for GJ 3021 and HD 169830, respectively. These measurements were obtained between HJD = 2 451 128 and HJD = 2 451 590 for GJ 3021 and between HJD = 2 451 296 and HJD = 2 451 668 for HD 169830. Table 5 provides the fitted orbital elements to these measurements as well as the computed minimum masses of the planetary companions and their semi-major axes. The radial-velocity are displayed in Fig. 2.

91 CORALIE radial-velocity measurements of HD 52265 have been gathered between HJD = 2 451 138 and HJD = 2 451 647. The mean photon-noise error of these velocities is 5.6 $\rm m\,s^{-1}$. During the first observing season, we found the orbital solution but we decided to wait for additional measurements to check the validity of this solution. The strange behaviour of some of the measurements of the second season pushed us to delay the announcement of the detection (see open triangles in Figs. 2c and 2d). Up to now, we still have no explanation for what happened between HJD = 2 451 430 and HJD = 2 451 500. We did not find this kind of behaviour on any other star in our sample and no instrumental problem was reported during this period. We decided at

Table 5. Fitted orbital elements for GJ 3021, HD 52265 and HD 169830 and characteristics of their planetary companions

Parameter	Units	GJ 3021	HD 52265	HD 169830
P	(days)	133.71 ± 0.20	119.6 ± 0.42	229.9 ± 4.6
T	(HJD − 2 400 000)	51 545.86 ± 0.64	51 422.3 ± 1.7	51 485.9 ± 4.8
e		0.511 ± 0.017	0.35 ± 0.03	0.35 ± 0.04
γ	($\mathrm{km\,s^{-1}}$)	−5.806 ± 0.003	53.769 ± 0.001	−17.215 ± 0.003
ω	(°)	290.7 ± 3.0	211 ± 6	183 ± 7
K_1	($\mathrm{m\,s^{-1}}$)	167 ± 4	42 ± 1	83 ± 4
$a_1 \sin i$	(10^{-4}AU)	17.6 ± 0.4	4.26 ± 0.15	16.4 ± 0.7
$f_1(m)$	($10^{-10}\mathrm{M_\odot}$)	412 ± 31	7.33 ± 0.08	113 ± 14
N_{meas}		61	71	35
$<\epsilon_{\mathrm{RV}}>^{\ddagger}$	($\mathrm{m\,s^{-1}}$)	8.2	5.6	5.5
$\sigma(O-C)$	($\mathrm{m\,s^{-1}}$)	19.2	7.3	9.2
χ^2		188.18	45.52	31.45
$\mathrm{P}(\chi^2)$		$<5{\cdot}10^{-7}$	0.968	0.344
$m_2 \sin i$	($\mathrm{M_{Jup}}$)	3.37 ± 0.09	1.05 ± 0.03	2.94 ± 0.12
a	(AU)	0.49	0.5	0.82
$d_{\mathrm{Periastron}}$	(AU)	0.25	0.325	0.54
d_{Apastron}	(AU)	0.75	0.675	1.1
$T_{\mathrm{equ}}{}^{\natural}$	(°K)	260–440	330–480	280–410

‡ Mean photon-noise error, ♮ Equilibrium temperature, Guillot et al. (1996)

the end not to use these measurements to fit the orbital solution and only 71 radial-velocity measurements have been finally used.

2.6. GJ 3021 radial-velocity residuals and X–ray emission

The residuals from the fitted orbit for GJ 3021 are abnormally large ($\mathrm{P}(\chi^2) < 5{\cdot}10^{-7}$, see Table 5). With a mean photon-noise uncertainty of $8.2\,\mathrm{m\,s^{-1}}$ and an assumed systematic error of $7\,\mathrm{m\,s^{-1}}$, the expected value is of the order of 10-11 $\mathrm{m\,s^{-1}}$. The extra-scatter is therefore of the order of 15-16 $\mathrm{m\,s^{-1}}$. GJ 3021 is an active star (see Sect. 2.4). It is well known (Saar et al. 1998; Santos et al. 2000e, 2001b, 2000b) that features on the surface of active stars (such as spots) induce radial-velocity variations ("jitter") due to line profile variations. The predicted jitter for a very active G dwarf is of the order of 15-20 $\mathrm{m\,s^{-1}}$ (Santos et al. 2000e, 2001b, 2000b). We have computed the bisectors of our observed CCFs (for detail, see Queloz et al. 2001) for GJ 3021. The bisector span is variable ($P(\chi^2) < 0.001$). The dispersion of the bisector span measurements is larger ($\simeq 24\,\mathrm{m\,s^{-1}}$) than the observed extra-scatter ($\simeq 15\,\mathrm{m\,s^{-1}}$). A weak correlation between the bisector span and the observed residuals is detected. The photon-noise errors affecting our span measurements (mean error value: $\simeq 16\,\mathrm{m\,s^{-1}}$) are too high to enable us to clearly establish this correlation. At this point, we cannot conclude that the abnormal radial-velocity residuals result from line profile variations for GJ 3021.

A correlation between rotation and X–ray emission is known to exist (see e.g Queloz et al. 1998). This correlation can be well illustrated using a $\log(L_{\mathrm{X}}/L_{\mathrm{Bol}})$ versus $\log(P_{\mathrm{rot}}/\tau_{\mathrm{c}}) - \log(\sin i)$ diagram (Rossby diagram). For GJ 3021, we have $\log(L_{\mathrm{X}}/L_{\mathrm{Bol}}) \simeq -4.4$. Using our measured $v \sin i$, $\log(\tau_{\mathrm{c}}) = 1.238$ (from the calibration in Noyes et al. 1984) and assuming a stellar radius of $R = 0.9\,\mathrm{R_\odot}$, we find $\log(P_{\mathrm{rot}}/\tau_{\mathrm{c}}) - \log(\sin i) = -0.320$. This value corresponds to the value expected for this $\log(L_{\mathrm{X}}/L_{\mathrm{Bol}})$ ratio (see Fig. 9 in Queloz et al. 1998). The X–ray emission of GJ 3021 probably results from activity-related processes.

3. The planetary companions around ι Hor, HD 210277 and HD 217107

In this section, we present the CORALIE measurements and orbital solutions for the solar-type stars ι Hor, HD 210277 and HD 217107.

3.1. The planetary companion of ι Hor

Indications of the potential presence of a planetary companion around the young solar-type star ι Hor (HD 17051, HIP 12653) were first presented during the summer 1998 by Kürster et al. (1998, 1999). During the summer 1999, these authors have published their final solution for the planetary companion (Kürster et al. 2000): a 320–day non-circular orbit with a radial-velocity semi-amplitude of $67\,\mathrm{m\,s^{-1}}$. Their inferred minimum mass for the companion is $m_2 \sin i = 2.26 \pm 0.18\,\mathrm{M_{Jup}}$ (assuming $M_1 = 1.03\,\mathrm{M_\odot}$).

3.1.1. CORALIE data and orbital solution for ι Hor

We have 26 CORALIE radial-velocity measurements of ι Hor. The time interval between the first and the last measurement is a little less than two orbital cycles (Δ t= 604 days) and we are able to compute our own orbital solution. The mean photon noise error of these mea-

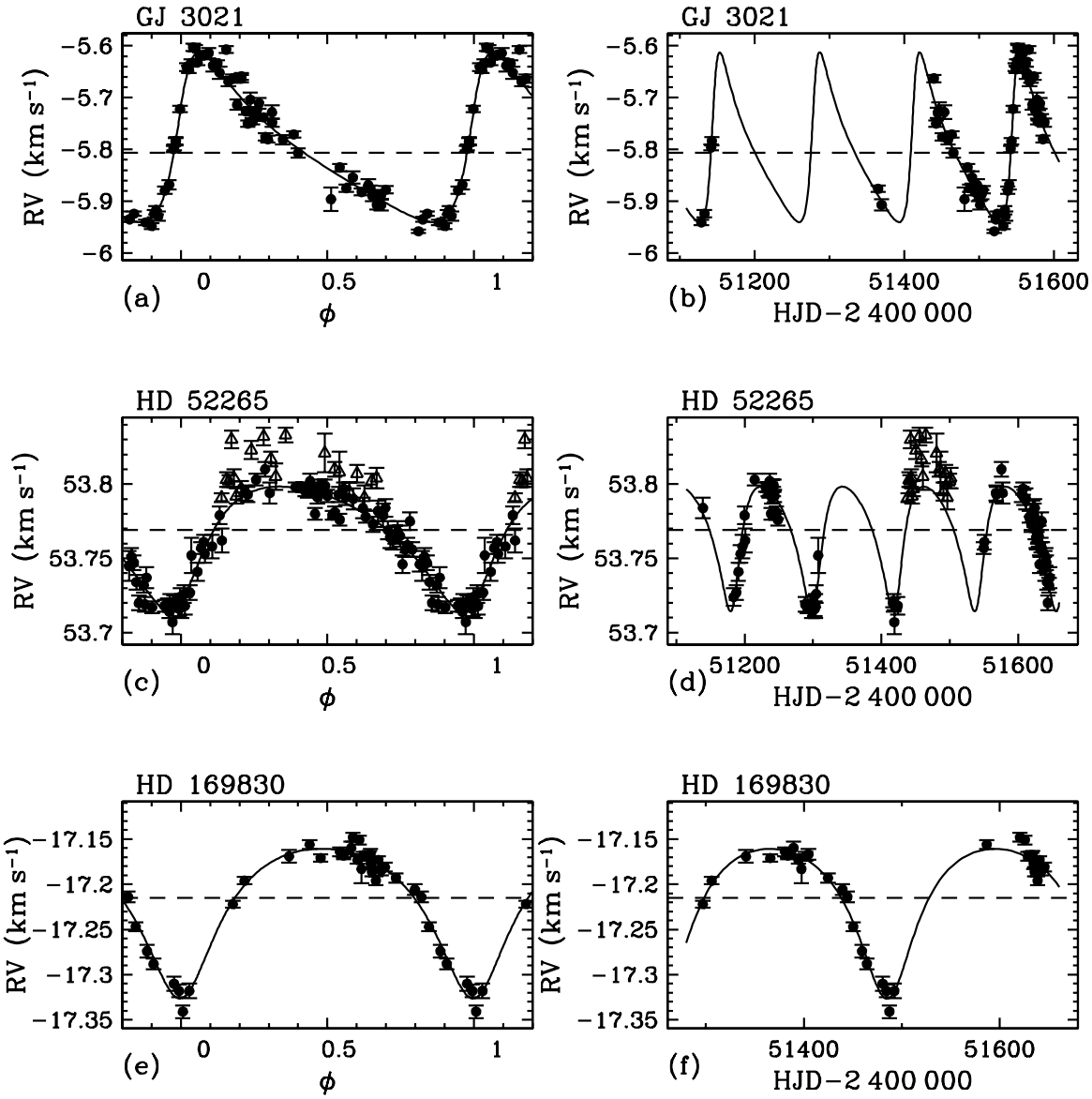

Fig. 2. CORALIE data: fitted orbital solutions for GJ 3021, HD 52265 and HD 169830. Left column: phase-folded velocities. Right Column: temporal velocities. The open triangles in panels **(c)** and **(d)** indicate measurements that have not been used for computing the orbital solution of HD 52265

surements is $6.5\,\mathrm{m\,s^{-1}}$. This rather high value for such a bright star ($m_\mathrm{V}=5.4$) is due to the rather large rotational velocity of ι Hor: $v\sin i = 6.1\pm1\,\mathrm{km\,s^{-1}}$ (CORAVEL data, calibration by Benz & Mayor 1984) in agreement with Saar & Osten (1997) who found $v\sin i = 5.7\pm0.5\,\mathrm{km\,s^{-1}}$. Table 6 lists our fitted orbital elements compared to those published by Kürster et al. (2000). We have fixed the orbital period to their value because of their much longer time coverage ($\simeq$ 6 cycles). Although our solution is a little bit different, CORALIE measurements are compatible with the solution by Kürster et al. (2000)[4]. The residuals from the fitted orbit obtained by imposing their period, eccentricity and semi-amplitude are $17\,\mathrm{m\,s^{-1}}$. Our orbital elements lead to a minimum planetary mass of $m_2\sin i = 2.41\pm0.18\,\mathrm{M_{Jup}}$ (assuming $M_1 = 1.03\,\mathrm{M_\odot}$). The residuals from the fitted orbit are abnormally large ($\sigma(O-C)$=16.6 $\mathrm{m\,s^{-1}}$, $\mathrm{P}(\chi^2)=6{\cdot}10^{-6}$). Assuming a typical intrinsic precision of $7\,\mathrm{m\,s^{-1}}$ for CORALIE and taking $6.5\,\mathrm{m\,s^{-1}}$ for the statistical error, the expected residuals value is $\sigma(O-C)\simeq10.3\,\mathrm{m\,s^{-1}}$ so the observed extra-scatter is of the order of $14\,\mathrm{m\,s^{-1}}$. These abnormally high residuals are also observed by Kürster et al. (2000). Their observed residuals are $27\,\mathrm{m\,s^{-1}}$ to be compared with their typical precision of $17\,\mathrm{m\,s^{-1}}$. ι Hor is chromospherically active: $\log(R'_{HK}) = -4.65$ (Henry et al. 1996). An excess scatter of $10-16\,\mathrm{m\,s^{-1}}$ is expected for this activity level

[4] Note that the T_0 published by Kürster et al. corresponds to the time of maximum radial velocity whereas our T is the time of closest approach. In our time system, the orbital phase of the maximum is $\phi=0.745$. We have: $T = T_0 + (0.255 + \mathrm{N_{cycles}})$. In our case, $\mathrm{N_{cycles}}=3$. The T value corresponding to their T_0 value is 51 348.9 in agreement with our value

and for this type of star (Saar et al. 1998; Santos et al. 2000e) so activity-related processes are probably responsible for the high residuals observed by both groups.

Figure 3a shows the CORALIE phase-folded curve with P fixed to 320.1 days. The temporal velocities with the same orbital solution are displayed in Fig. 3c.

3.1.2. Combined orbital solution

We present the orbital solution we obtain for ι Hor after combining the CORALIE measurements with the velocities obtained by Kürster et al. (2000). The mean uncertainty of their radial velocities is about $17.5\,\mathrm{m\,s^{-1}}$ a much larger value than the $6.5\,\mathrm{m\,s^{-1}}$ of the CORALIE measurements. We used only the best Kürster et al. velocities for fitting the combined orbit (data points with $\epsilon_{\mathrm{RV}} < 20\,\mathrm{m\,s^{-1}}$). 62 measurements matched this criterion. Kürster et al. measurements are differential velocities (velocity difference between the observed spectra and a reference spectra) so they have an arbitrary systemic velocity. Our computed combined orbital solution included the velocity offset between the two sets of data as an additional free parameter. The fitted offset is (C: CORALIE, K: Kürster): $\Delta\mathrm{RV} = \mathrm{RV_C} - \mathrm{RV_K} = 16.910 \pm 0.010\ \mathrm{km\,s^{-1}}$.

Table 6 provides the fitted combined orbital solution. Figure 3b shows the combined phase-folded curve. The temporal velocities with the combined solution are displayed in Fig. 3d. The computed planetary minimum mass in this case is $m_2 \sin i = 2.24 \pm 0.13\,\mathrm{M_{Jup}}$[5].

3.2. The planetary companion of HD 210277

The presence of a planetary companion orbiting the late G dwarf HD 210277 has been announced a few years ago by Marcy et al. (1999). In a recent paper, Vogt et al. (2000) have presented an updated version of the orbital solution. To obtain this new orbit, these authors have added new measurements with the HIRES spectrograph (Vogt et al. 1994) on the KECK telescope. Improvements in their reduction software have also increased their precision. Our 42 radial-velocity measurements are compatible with the orbital solution by Vogt et al. (2000).

3.2.1. CORALIE data for HD 210277

42 CORALIE radial velocities of HD 210277 were measured between HJD =2 451 064 and HJD =2 451 497. The mean photon noise error of these measurements is $6\,\mathrm{m\,s^{-1}}$. With 433 days between the first and the last measurement, our time span is a little shorter than the orbital period published by Vogt et al. (436.6 days) so we do not have a reliable constraint on the periodicity of the system. We choose to set $P = 436.6$ days as a fixed parameter in our fit. Table 7 shows our fitted orbital solution compared to the one by Vogt et al. (2000). There are some small differences between the two solutions (larger semi-amplitude and smaller eccentricity for the CORALIE solution) but they are mostly due to our poor phase coverage (no data point at the phase of the maximum radial velocity). If we set constant in the fit all the orbital elements by Vogt et al. (except for the γ velocity which we keep as a free parameter), we obtain a very good agreement between our data and their solution. We find $\sigma(O-C) = 7.7\,\mathrm{m\,s^{-1}}$ to be compared with the $7.5\,\mathrm{m\,s^{-1}}$ obtained fixing only the period. Assuming $0.92\,\mathrm{M_\odot}$ for the mass of the primary (Gonzalez et al. 1999), we find a planetary minimum mass of $m_2 \sin i = 1.73 \pm 0.29\,\mathrm{M_{Jup}}$, a value significantly higher than the one found by Vogt et al. ($1.23\,\mathrm{M_{Jup}}$). This difference is due to the difference in the velocity semi-amplitude ($52\,\mathrm{m\,s^{-1}}$ for CORALIE, $39\,\mathrm{m\,s^{-1}}$ for HIRES).

Figure 3e shows the phase-folded curve obtained in this case for HD 210277. The temporal velocities with the same orbital solution are displayed in Fig. 3g.

3.2.2. Combined orbital solution

In order to obtain better constraints on the orbital elements, we have combined the CORALIE data with the HIRES radial-velocity measurements by Vogt et al. (2000). As for the Kürster et al. (2000) velocities, the Vogt et al. measurements are differential velocities so they have an arbitrary systemic velocity. We first fitted their systemic velocity (Keplerian fit with γ as the only free parameter, other parameters fixed to the Vogt et al. values). We made the same computation with the CORALIE velocities in order to compute the velocity offset between the two sets of data. We found (C: CORALIE, V: Vogt et al.): $\mathrm{RV_C} = \mathrm{RV}_V - 20.930\ \mathrm{km\,s^{-1}}$

The combined orbital solution, whose results are presented in Table 7, was obtained by fitting a Keplerian orbit to the combined data (CORALIE + corrected HIRES velocities). We checked our velocity correction by fitting the velocity offset (additional free parameter). The fitted residual offset is smaller than $0.5\,\mathrm{m\,s^{-1}}$. The computed minimum mass is $m_2 \sin i = 1.24 \pm 0.03\,\mathrm{M_{Jup}}$. Figure 3 shows the phase-folded-curve (panel f) and the velocities as a function of time (panel h) for the CORALIE + HIRES combined solution.

3.3. The planetary companion of HD 217107

The discovery of a planetary companion orbiting the G7 dwarf HD 217107 was initially announced by Fischer et al. (1999). This discovery was based on radial velocities obtained with the HAMILTON echelle spectrometer (Vogt 1987) at Lick Observatory and with the HIRES echelle spectrometer (Vogt et al. 1994) on the KECK telescope.

[5] The combined orbital solution has a more uncertain periastron epoch than the Kürster et al. time of maximum radial-velocity. We fitted the orbital solution to the Kürster et al. velocities using our software. We obtained a solution compatible with the Kürster et al. published solution but with a 12 days uncertainty on this parameter. The difference between the uncertainties is possibly due to differences in the fitting processes

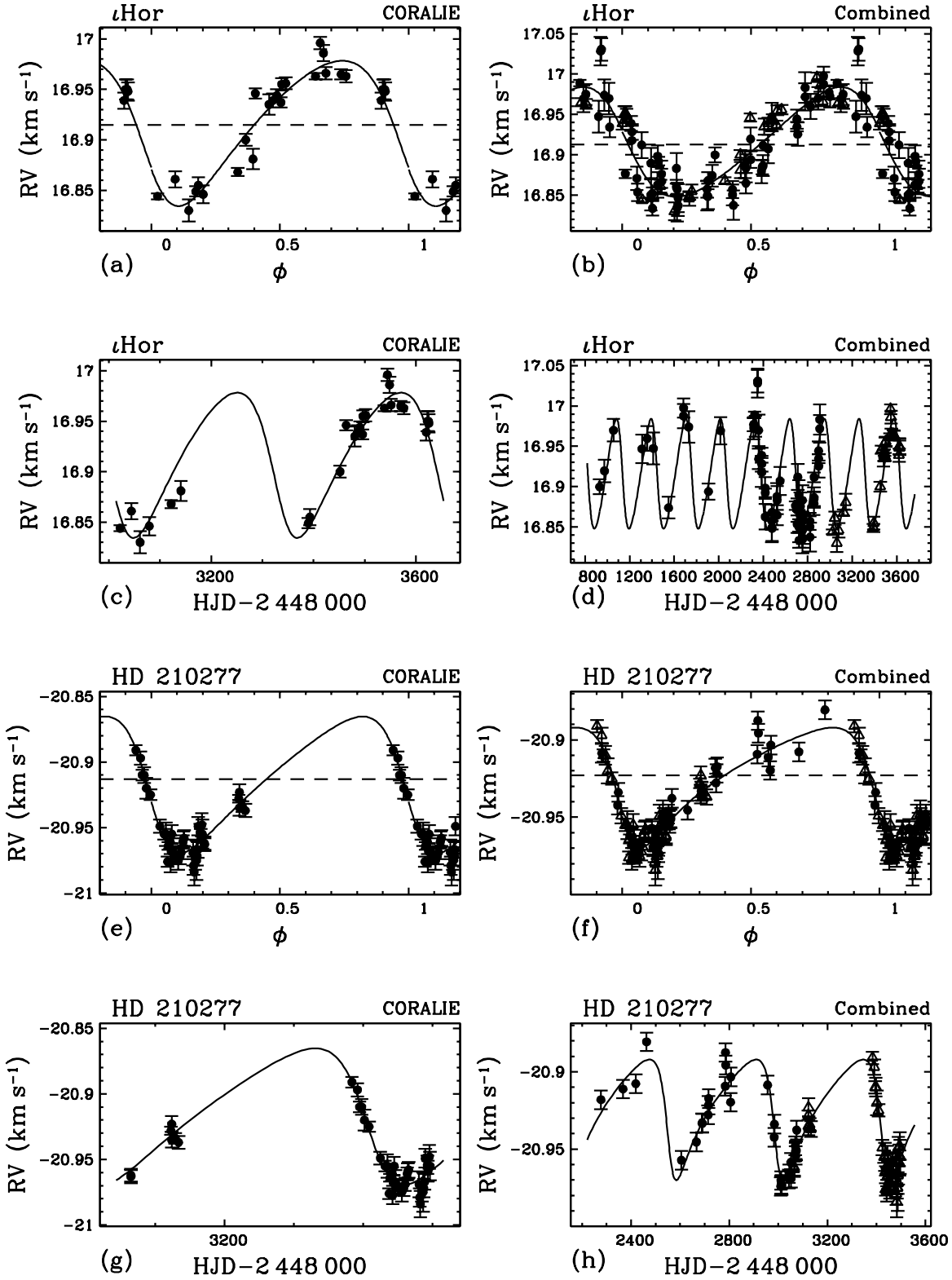

Fig. 3. Phase-folded curves and temporal radial velocities for ι Hor and HD 210277. Left column: CORALIE orbital solutions. Right column: combined orbital solutions. **(b)** and **(d)**: CORALIE (open triangles) and Kürster et al. (2000, filled dots). **(f)** and **(h)**: CORALIE (open triangles) and Vogt et al. (2000, filled dots)

In a recent paper, Vogt et al. (2000) have presented updated orbital elements for this planet. This orbit was based on radial-velocity measured with the HIRES spectrometer (Vogt et al. 1994) and agreed with the orbital solution from the discovery paper. Vogt et al. (2000) also announced the discovery of a linear drift of the systemic velocity with a slope of 39.4 ± 3.5 m s^{-1} yr^{-1}. This trend was later confirmed by Fischer et al. using their

Table 6. Orbital elements for ι Hor. Results by Kürster et al. (2000) are shown for comparison. The orbital solution combining CORALIE (C) and Kürster et al. (K) data is also presented. T_{max} is the time of maximum radial velocity

Parameter	Units	CORALIE	Kürster et al.	Combined Solution
P	(days)	320.1 (fixed)	320.1 ± 2.1	311.3 ± 1.3
T	(HJD − 2 400 000)	51 334 ± 14	...	51 308.8 ± 10.4
T_{max}	(HJD − 2 400 000)	...	50 307.0 ± 3.0	...
e		0.25 ± 0.07	0.161 ± 0.069	0.22 ± 0.06
γ	($km\,s^{-1}$)	16.915 ± 0.003	...	16.913 ± 0.003
ω	(°)	119 ± 77	83 ± 11	78.9 ± 13.1
K_1	($m\,s^{-1}$)	72 ± 5	67.0 ± 5.1	68 ± 4
$a_1 \sin i$	(10^{-3}AU)	2.06 ± 0.15	1.94 ± ...	1.88 ± 0.11
$f_1(m)$	($10^{-9} M_\odot$)	11.5 ± 2.5	9.5 ± ...	9.5 ± 1.6
$m_2 \sin i$	(M_{Jup})	2.41 ± 0.18	2.26 ± 0.18	2.24 ± 0.13
N_{meas}		26	95	88 (C:26, K:62)
$\sigma(O-C)$	($m\,s^{-1}$)	16.6	27.0	23.2 (C:20.2, K:24.3)
χ^2		62.15	...	186.87
P(χ^2)		$6{\cdot}10^{-6}$	...	$< 5{\cdot}10^{-7}$

Table 7. Orbital elements for HD 210277. Results by Vogt et al. (2000) are shown for comparison. The orbital solution combining CORALIE (C) and Vogt et al. (V) data is also presented

Parameter	Units	CORALIE	Vogt et al.	Combined Solution
P	(days)	436.6 (fixed)	436.6 ± 4	435.6 ± 1.9
T	(HJD − 2 400 000)	51 410 ± 13	51 428 ± 4	51 426.4 ± 2.5
e		0.342 ± 0.055	0.45 ± 0.03	0.450 ± 0.015
γ	($km\,s^{-1}$)	−20.913 ± 0.006	... ± ...	−20.923 ± 0.001
ω	(°)	104 ± 13	118 ± 6	117.4 ± 3.3
K_1	($m\,s^{-1}$)	52 ± 9	39 ± 2	39 ± 1
$a_1 \sin i$	(10^{-3}AU)	1.96 ± 0.33	1.39 ± ...	1.40 ± 0.03
$f_1(m)$	($10^{-9} M_\odot$)	5.3 ± 2.7	1.91 ± ...	1.97 ± 0.13
$m_2 \sin i$	(M_{Jup})	1.73 ± 0.29	1.23 ± ...	1.24 ± 0.03
N_{meas}		42	45	87 (C:42, V:45)
$\sigma(O-C)$	($m\,s^{-1}$)	7.5	3.24	6.10 (C:8.23, V:3.23)
χ^2		24.45	...	61.59
P(χ^2)		0.944	...	0.937

Table 8. Orbital elements for HD 217107. Results by Vogt et al. (2000) are shown for comparison. The systemic drift was taken into account in both cases. The orbital solution combining CORALIE data (C) with the measurements by Fischer et al. (1999) (F) and Vogt et al. (2000) (V) is also presented. There are no significant differences between these solutions

Parameter	Units	CORALIE Time bins	Vogt et al. Linear correction	Combined solution Time bins
P	(days)	7.1260 ± 0.0005	7.1260 ± 0.0007	7.1262 ± 0.0003
T	(HJD − 2 400 000)	51 452.388 ± 0.079	51 331.4 ± 0.2	51 452.477 ± 0.056
e		0.126 ± 0.009	0.140 ± 0.02	0.134† ± 0.007
γ	($km\,s^{-1}$)	−13.413♮ ± 0.001	... ± ...	−13.413♮ ± 0.001
ω	(°)	24 ± 4	31 ± 7	29 ± 3
K_1	($m\,s^{-1}$)	140 ± 1	140 ± 3	140 ± 1
$a_1 \sin i$	(10^{-5}AU)	9.1 ± 0.1	9.1 ± ...	9.07 ± 0.07
$f_1(m)$	($10^{-9} M_\odot$)	1.96 ± 0.06	1.97 ± ...	1.99 ± 0.04
$m_2 \sin i$	(M_{Jup})	1.275 ± 0.013	1.28 ± 0.4	1.282 ± 0.009
N_{meas}		63	21	98 (C:63, F:14, V:21)
$\sigma(O-C)$	($m\,s^{-1}$)	7.0	4.2	7.21 (C:7.40, F:10.18, V:3.73)

† highly significant according to the Lucy & Sweeney test (Lucy & Sweeney 1971)
♮ at HJD = 2 451 450 (= median of the third CORALIE time bin)

most recent observations (slope = 43.3 ± 2.8 $m\,s^{-1}\,yr^{-1}$). In Sect. 3.3.1, we present the CORALIE radial-velocity measurements and orbital solution for HD 217107 confirming the orbital solutions by Fischer et al. (1999) and Vogt

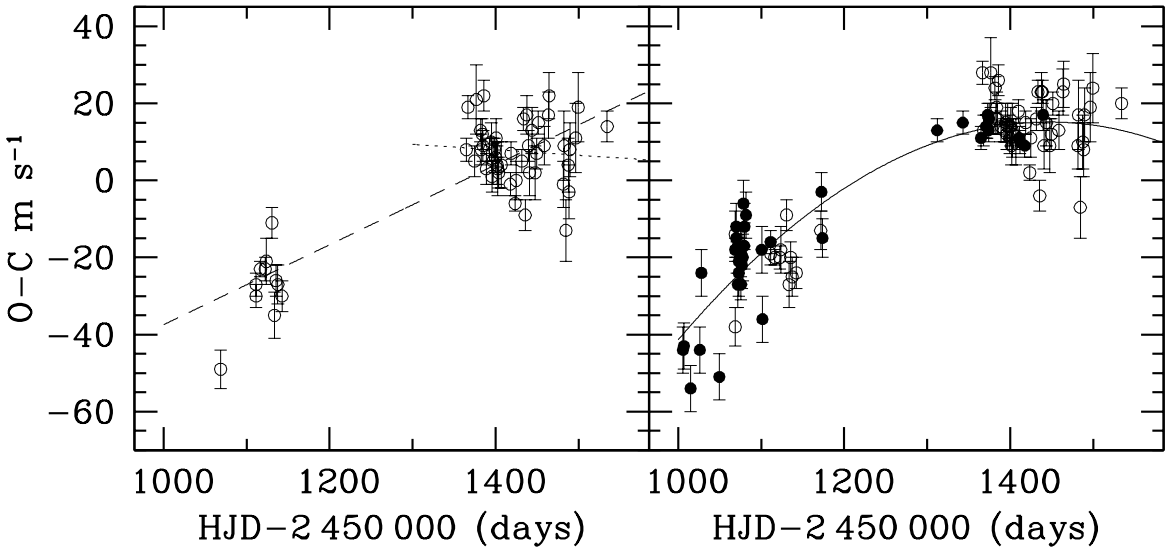

Fig. 4. Left: CORALIE data. Residuals versus time. The orbital solution by Vogt et al. (2000) has been used. Only our 58 best measurements are plotted. A linear fit to these residuals gives a slope of 37.9 ± 3.4 m s^{-1} yr^{-1} (dashed line). A linear fit to the most recent data (data from the last observing season only) gives a slope of -5 $\pm$ 10 m s^{-1} yr^{-1} (dotted line). This difference between the two slopes tend to indicate a non-linear trend. Right: residual from the combined orbit (see Table 8) of HD 217107. Open dots: CORALIE data, Filled dots: Vogt et al. (2000) and Fischer et al. (1999) data. The curve shows the result of a quadratic fit to these residuals. The fitted function is: $O-C(\tau) = K_0 + K_1\tau + K_2\tau^2$ where $\tau = \text{HJD} - 2\,450\,000$. The quadratic term is significant: $K_2 = -2.83 \pm 0.54$ (10^{-4} m s^{-1} d^{-2}). The χ^2 statistics shows that a linear trend is very unlikely (see Table 10)

et al. (2000). We also confirm the γ velocity drift revealing the presence of a third massive body in the system. We show that this drift is probably not linear. An orbital solution combining all the available data is presented in Sect. 3.3.2.

3.3.1. CORALIE data for HD 217107

In this section we present the CORALIE data for HD 217107. We shall focus on the systemic velocity drift correction in order to adjust the best orbital solution.

63 CORALIE radial-velocity measurements have been gathered during the first two observing seasons (1998–1999). These velocities span from HJD = 2 451 538 to HJD = 2 451 067) and have a mean photonic error of 5.5 m s^{-1}.

We first imposed the solution by Vogt et al. (2000) to our 58 best measurements to see the behaviour of the residuals (we only fitted the γ velocity). The residuals obtained from this solution are 16.1 m s^{-1}, a clearly abnormally high value.

Figure 4 (left) shows the residuals as a function of time. A trend is clearly visible. A linear fit to the residuals of the two seasons gives a slope of 37.9 ± 3.4 m s^{-1} yr^{-1} (compatible with the previously detected trends). A linear fit to the residuals of the last observing season (HJD > 2 451 300) gives a slope of -5 ± 10 m s^{-1} yr^{-1} (consistent with zero). These two slope values are not compatible. The slope difference is not highly significant ($P(\chi^2) = 0.29$ and 0.85, respectively for the last season measurements). At this point and using the CORALIE data alone, there are only clues indicating that the drift is not linear over the two seasons.

The CORALIE orbital solution presented in Table 8 was obtained after correcting the γ velocity drift using a time bins correction. We split our data into three time bins (see Table 9). We fit a Keplerian orbit to the data in the third time bin. We fit the systemic velocity of the second time bin (Keplerian fit with γ as the only free parameter, other parameters fixed to the fitted values for the third time bin). We correct the velocities of the second time bin so that they have the same systemic velocity as the velocities of the third time bin. We then fit a new Keplerian orbit to the velocities of the third time bin plus the corrected velocities of the second time bin. We correct the velocities of the first time bin using the same procedure. Once all the bins are corrected, we fit a Keplerian orbit to the full set of data. With this kind of drift correction, we do not have to make any assumption on the drift shape. The residuals from the fitted solution (7 m s^{-1}) are compatible with the typical precision of CORALIE. We also computed an orbital solution using a linear correction. The residual from this solution are substantially higher: 9.1 m s^{-1}.

In Table 8 are listed the fitted parameters for the time bins correction. The orbital solution by Vogt et al. (2000), is shown for comparison. There are no substantial differences between these solutions. Assuming a primary mass $M_1 = 0.96\,M_\odot$ (similarly to Fischer et al. 1999), the computed minimum mass is $m_2 \sin i = 1.275 \pm 0.013\,M_{\rm Jup}$.

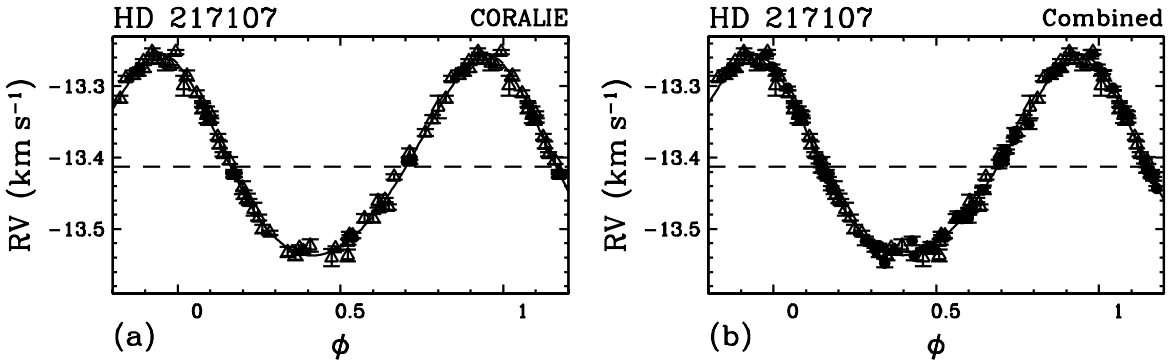

Fig. 5. Left: CORALIE phase-folded curve. Right: CORALIE, Vogt et al. (2000) and Fischer et al. (1999) combined phase-folded curve. A time bins correction has been used in both cases. A linear fit to the residuals around these two orbital solutions gives a flat slope

Table 9. Time bins correction for the CORALIE measurements and for the data by Fischer et al. (1999) and Vogt et al. (2000). All the velocities are in $\mathrm{km\,s^{-1}}$

$\mathbf{JD}^{\dagger}_{\mathrm{min}}$	$\mathbf{JD}^{\dagger}_{\mathrm{max}}$	$\mathbf{N}_{\mathrm{meas}}$	γ	$\mathbf{\Delta RV}^{\ddagger}$
CORALIE				
67	69	2	-13.473 ± 0.012	0.060
111	143	10	-13.448 ± 0.002	0.035
364	538	51	-13.413 ± 0.001	0
Fischer et al. (1999)				
5	50	6	0.042 ± 0.004	-13.455
76	102	8	0.068 ± 0.004	-13.481
Vogt et al. (2000)				
68	76	7	-0.004 ± 0.002	-13.409
171	174	3	0.004 ± 0.003	-13.417
312	375	7	0.029 ± 0.001	-13.442
410	439	4	0.030 ± 0.002	-13.443

† JD = HJD − 2 451 000.
‡ Correction to set the velocities into the systemic velocity of the third CORALIE time bin

Table 10. χ^2 statistics for the different types of γ velocity correction for HD 217107. $N_{\mathrm{d.of.f}}$ is the number of degrees of freedom

Correction	N_{param}	$N_{\mathrm{d.of.f}}$	χ^2	$\mathbf{P}(\chi^2)$
Time bins	14	84	68.37	0.892
Quadratic	10	88	107.91	0.074
Linear	9	89	405.73	$< 5{\cdot}10^{-7}$

Figure 5a shows the CORALIE phase-folded curve for the time bins correction.

3.3.2. Combined orbital solution

In order to improve the precision on the orbital elements, we computed a combined orbital solution using the CORALIE data, the velocities by Fischer et al. (1999) and the velocities by Vogt et al. (2000). Before computing the combined orbital solution, we had to bring the different sets of data into a common velocity system. We decided to set all the velocities into the CORALIE γ velocity at HJD = 2 451 450 reference frame (median of the third time bin, see Sect. 3.3.1). We applied a time bins correction for the data by Fischer et al. (1999) and by Vogt et al. (2000) in order to remove simultaneously the systemic drift effect and the radial-velocity offsets (differential velocities) between the different instruments.

The fitted orbital elements for the combined solution are listed in Table 8. The computed minimum mass of the planet is $m_2 \sin i = 1.282 \pm 0.009\,\mathrm{M_{Jup}}$. Constraining the eccentricity to be zero causes the residuals to increase to $14.4\,\mathrm{m\,s^{-1}}$ indicating that the non-zero eccentricity is highly significant. The confidence level as computed with the Lucy & Sweeney test (Lucy & Sweeney 1971) is almost 100 %. Figure 5b shows the phase-folded curve for the combined orbital solution.

Using the uncorrected data, we now want to describe more precisely the shape of the systemic drift. We first have to set all the available data into the same velocity system. A time bins correction can not be used in this case because it cancels out all the γ velocity information (instrumental offsets and drift effect). The offset between the velocities by Fischer et al. (1999) and Vogt et al. (2000) is corrected using 7 measurements present in the two data sets. The offset between the CORALIE and the Vogt et al. (2000) velocities is obtained by computing a combined orbital solution using data taken during a common epoch (namely, the beginning of the second season) with the offset as an additional free parameter. We have (C: CORALIE, F: Fischer et al., V: Vogt et al.):

$$RV_{\mathrm{V}} = RV_{\mathrm{F}} - 70.5 \pm 2.3\,\mathrm{m\,s^{-1}}$$
$$RV_{\mathrm{C}} = RV_{\mathrm{V}} - 13.442 \pm 0.010\,\mathrm{km\,s^{-1}}$$

All the velocities have been finally set into the CORALIE system. Figure 4 (right) shows the residuals from the combined orbit (the combined orbit of Table 8 has been used with the γ velocity as the only free parameter). The velocity drift is clearly not linear. A quadratic fit to these residuals has been computed and is also plotted in Fig. 4 (right, solid line). The second order term of this fit is significant: $-2.83 \pm 0.54\,(10^{-4}\,\mathrm{m\,s^{-1}\,d^{-2}})$. The available data

do not give a reliable constraint on the mass of the third body of the system. For the moment, a companion within the planetary mass range cannot be ruled out.

Finally, if we fit a Keplerian orbit to the velocities corrected for the quadratic drift, we end up with a solution compatible with the combined solution of Table 8. The residuals from this solution are $8.86\,\mathrm{m\,s^{-1}}$. Table 10 shows the values of the χ^2 statistics for the different corrections of the γ velocity drift. The huge difference in $\mathrm{P}(\chi^2)$ between the linear and the quadratic corrections shows that a linear drift is very unlikely.

4. Conclusion

In this paper, we presented our CORALIE radial-velocity measurements for the 6 stars GJ 3021, HD 52265, HD 169830, ι Hor, HD 210277 and HD 217107. We reported the detection of 3 new planetary companions orbiting the solar type stars GJ 3021, HD 52265 and HD 169830. These planets have longer periods than the "Hot Jupiters" (the periods are respectively 133.7, 119.2 and 229.9 days). All the fitted orbits are elongated (the eccentricities are respectively 0.51, 0.35 and 0.35). They are all Jovian planets (the minimum masses are respectively 3.37, 1.05 and $2.94\,\mathrm{M_{Jup}}$). Using CORALIE data, we have estimated the chromospheric activity level of these candidates. GJ 3021 is a very active star whereas HD 52265 and HD 169830 are quiescent. The high activity level of GJ 3021 is probably responsible for the high residuals from the fitted orbit. We also estimated the Lithium abundances of these stars using CORALIE spectra. GJ 3021 and HD 52265 exhibit a strong λ 6707.8 Å Li I absorption feature whereas no Lithium is detected for HD 169830. The 3 stars have a higher metal content than the Sun. The spatial velocities of GJ 3021, its metallicity, its chromospheric activity level and its Lithium abundance are consistent with the values observed for members of the Hyades Super-Cluster.

We confirmed the orbital solution by Kürster et al. (2000) for ι Hor and the solutions by Vogt et al. (2000) for HD 210277 and HD 217107. For the latter, we also confirmed the systemic velocity drift showing it is probably not linear over our first two observing seasons. Finally, we computed combined orbital solutions for these 3 stars using all the available velocity measurements improving the precision on the orbital elements.

Acknowledgements. We acknowledge support from the Swiss National Research Foundation (FNRS) and from the Geneva university. Support from Fundação para a Ciência e Tecnologia, Portugal, to N.C.S. in the form of a scholarship is gratefully acknowledged. We wish to thank Fabien Carrier, Francesco Kienzle, Claudio Melo and Frederic Pont for additional measurements obtained during their own observing runs. This research has made use of the SIMBAD database, operated at CDS, Strasbourg, France.

References

Baranne, A., Queloz, D., Mayor, M., et al. 1996, A&AS, 119, 373
Benz, W. & Mayor, M. 1984, A&A, 138, 183
Butler, R. P., Marcy, G. W., Fischer, D. A., et al. 1999, ApJ, 526, 916
Butler, R. P., Vogt, S. S., Marcy, G. W., et al. 2000, ApJ, 545, 504
Charbonneau, D., Brown, T. M., Latham, D. W., & Mayor, M. 2000, ApJ, 529, L45
Chereul, E., Crézé, M., & Bienaymé, O. 1999, A&A, 135, 5
Cochran, W. D., Hatzes, A. P., Butler, R. P., & Marcy, G. W. 1997, ApJ, 483, 457+
Decin, G., Dominik, C., Malfait, K., Mayor, M., & Waelkens, C. 2000, A&A, 357, 533
Donahue, R. 1993, PhD thesis, New Mexico State University
Edvardsson, B., Andersen, J., Gustafsson, B., et al. 1993, A&A, 275, 101+
ESA. 1997, The HIPPARCOS and TYCHO catalogue, ESA-SP 1200
Fischer, D. A., Marcy, G. W., Butler, R. P., Vogt, S. S., & Apps, K. 1999, PASP, 111, 50
Fischer, D. A., Marcy, G. W., Butler, R. P., et al. 2001, ApJ, 551, 1107
Flower, P. J. 1996, ApJ, 469, 355+
Gonzalez, G. 2000, in ASP Conf. Ser., Vol. 219, Planetesimals and Planets, ed. F. Garzón, C. Eiroa, D. de Winter, & T. Mahoney, 523–533
Gonzalez, G., Wallerstein, G., & Saar, S. H. 1999, ApJ, 511, L111
Guillot, T., Burrows, A., Hubbard, W. B., Lunine, J. I., & Saumon, D. 1996, ApJ, 459, L35
Henry, G. W., Marcy, G. W., Butler, R. P., & Vogt, S. S. 2000, A&A, 529, L41
Henry, T. J., Soderblom, D. R., Donahue, R. A., & Baliunas, S. L. 1996, AJ, 111, 439+
Hünsch, M., Schmitt, J. H. M. M., Sterzik, M. F., & Voges, W. 1999, A&AS, 135, 319
Kürster, M., Endl, M., Els, S., et al. 2000, A&A, 353, L33
Kürster, M., Hatzes, A., Cochran, W., et al. 1998, in Workshop Science with Gemini, ed. B. Barbuy, E. Lapasset, R. Batista, & R. Cid Fernandes, IAG-USP & UFSC
Kürster, M., Hatzes, A., Cochran, W., et al. 1999, in PASP Conf. Ser., Vol. 185, IAU Colloq. 170, ed. J. Hearnshaw & C. Scarfe, 154
Lucy, L. B. & Sweeney, M. A. 1971, AJ, 76, 544+
Marcy, G. W., Butler, R. P., & Vogt, S. S. 2000, ApJ, 536, L43
Marcy, G. W., Butler, R. P., Vogt, S. S., Fischer, D., & Liu, M. C. 1999, ApJ, 520, 239
Mayor, M., Naef, D., Pepe, F., et al. 2000, in Planetary Systems in the Universe: Observations, Formation and Evolution, ed. A. Penny, P. Artymowicz, A.-M. Lagrange, & S. Russell, ASP Conf. Ser.

Mayor, M. & Queloz, D. 1995, Nat, 378, 355+
Naef, D., Latham, D., Mazeh, T., et al. 2001, A&A, in press
Naef, D., Mayor, M., Pepe, F., et al. 2000, in ASP Conf. Ser., Vol. 219, Planetesimals and Planets, ed. F. Garzón, C. Eiroa, D. de Winter, & T. Mahoney, 602–606
Ng, Y. K. & Bertelli, G. 1998, A&A, 329, 943
Noyes, R. W., Hartmann, L. W., Baliunas, S. L., Duncan, D. K., & Vaughan, A. H. 1984, ApJ, 279, 763
Piters, A. J. M., van Paradijs, J., & Schmitt, J. H. M. M. 1998, A&AS, 128, 29
Queloz, D., Allain, S., Mermilliod, J. ., Bouvier, J., & Mayor, M. 1998, A&A, 335, 183
Queloz, D., Eggenberger, A., Mayor, M., et al. 2000a, A&A, 359, L13
Queloz, D., Henry, G., Sivan, J., et al. 2001, A&A, submitted
Queloz, D., Mayor, M., Naef, D., et al. 2000b, in Planetary Systems in the Universe: Observations, Formation and Evolution, ed. A. Penny, P. Artymowicz, A.-M. Lagrange, & S. Russell, ASP Conf. Ser.
Queloz, D., Mayor, M., Naef, D., et al. 2000c, in From extrasolar planets to cosmology: the VLT opening symposium, ed. J. Bergeron & A. Renzini, ESO Astrophysics Symposia Ser. (Heidelberg: Springer Verlag), 571
Queloz, D., Mayor, M., Weber, L., et al. 2000d, A&A, 354, 99
Saar, S. H., Butler, R. P., & Marcy, G. W. 1998, ApJ, 498, L153
Saar, S. H. & Osten, R. A. 1997, MNRAS, 284, 803
Santos, N., Israelian, G., & Mayor, M. 2000a, in Planetary Systems in the Universe: Observations, Formation and Evolution, ed. A. Penny, P. Artymowicz, A.-M. Lagrange, & S. Russell, ASP Conf. Ser.
Santos, N., Mayor, M., Naef, D., et al. 2000b, in Planetary Systems in the Universe: Observations, Formation and Evolution, ed. A. Penny, P. Artymowicz, A.-M. Lagrange, & S. Russell, ASP Conf. Ser.
Santos, N., Mayor, M., Naef, D., et al. 2001a, in ASP Conf. Ser., Vol. 223, the 11th. Cambridge Workshop on Cool Stars, Stellar Systems and the Sun, ed. R. García Lopez, R. Rebolo, & M. Zapatero Osorio
Santos, N., Mayor, M., Naef, D., et al. 2001b, in ASP Conf. Ser., Vol. 223, the 11th. Cambridge Workshop on Cool Stars, Stellar Systems and the Sun, ed. R. García Lopez, R. Rebolo, & M. Zapatero Osorio
Santos, N. C., Israelian, G., & Mayor, M. 2000c, A&A, 363, 228
—. 2001c, A&A, 373, 1019
Santos, N. C., Mayor, M., Naef, D., et al. 2000d, A&A, 356, 599
—. 2000e, A&A, 361, 265
Schaerer, D., Charbonnel, C., Meynet, G., Maeder, A., & Schaller, G. 1993, A&AS, 102, 339+
Soderblom, D. R., Jones, B. F., Balachandran, S., et al. 1993, AJ, 106, 1059
Udry, S., Mayor, M., Naef, D., et al. 2000a, A&A, 356, 590
Udry, S., Mayor, M., & Queloz, D. 2000b, in Planetary Systems in the Universe: Observations, Formation and Evolution, ed. A. Penny, P. Artymowicz, A.-M. Lagrange, & S. Russell, ASP Conf. Ser.
Udry, S., Mayor, M., Queloz, D., Naef, D., & Santos, N. 2000c, in From extrasolar planets to cosmology: the VLT opening symposium, ed. J. Bergeron & A. Renzini, ESO Astrophysics Symposia Ser. (Heidelberg: Springer Verlag), 571
Vaughan, A. H., Preston, G. W., & Wilson, O. C. 1978, PASP, 90, 267
Vogt, S. S. 1987, PASP, 99, 1214
Vogt, S. S., Allen, S. L., Bigelow, B. C., et al. 1994, Proc. SPIE, 2198, 362
Vogt, S. S., Marcy, G. W., Butler, R. P., & Apps, K. 2000, ApJ, 536, 902